Printed Sensors for Smart Objects in Industry 4.0

Michela Borghetti
Department of Information Engineering
University of Brescia
Brescia, Italy
michela.borghetti@unibs.it

Edoardo Cantù
Department of Information Engineering
University of Brescia
Brescia, Italy
e.cantu@unibs.it

Emilio Sardini
Department of Information Engineering
University of Brescia
Brescia, Italy
emilio.sardini@unibs.it

Mauro Serpelloni
Department of Information Engineering
University of Brescia
mauro.serpelloni@unibs.it

***Abstract*—With the advent of the fourth industrial revolution or Industry 4.0, manufacturing processes are undergoing radical changes thanks to the adoption of enabling technologies, such as Internet of Things (IoT), Big Data, Additive Manufacturing (AM), and Cloud Computing. As such, sensors are becoming essential to obtain additional data on production, parts, equipment health, and environmental conditions. All this concerns the aim of improving many aspects of industrial processes (flexibility, efficiency, cost, etc.). Sensors need to be placed everywhere in the industrial work environment (on machines, smart devices, objects, and tools) to monitor in real-time physical quantities such as temperature, vibrations, deformations that could affect production. With its characteristics, printed electronics (PE) can allow us the production of customized sensors and systems to make "smart" conventional objects. This work aims to analyze an innovative PE technology - aerosol printing - as manufacturing technology for electronics and sensors to be integrated into objects, showing examples of sensors fabricated by PE as applications that will be adopted for smart objects and Industry 4.0.**

Keywords— aerosol jet printing; photonic curing; flash lamp annealing; industry 4.0; I4.0; IoT; smart devices; predictive maintenance; environmental parameters monitoring.

I. INTRODUCTION

The fourth industrial revolution, also known as Industry 4.0 (I4.0) has started changing the traditional manufacturing systems, turning a conventional factory into a smart one. Smart factories are characterized by a complete connection between objects, machines, tools, and workers thanks to the so-called enabling technologies: Big Data, Internet of Things (IoT), Additive Manufacturing (AM), and Cloud Computing. In such a way, real-time monitoring could be provided improving efficiency and productivity, reducing costs thanks to proper predictability and also operators workload [1], [2].

Becoming context-aware devices, machines can collect data realizing a sensing network interacting with operators [3], [4]. In light of this, Industrial IoT (IIoT) is a network of intelligent industrial smart objects and devices that contributes to improving the flexibility and production rate, for a high level of control on processes and operational time. This is possible thanks to the capability to measure and check different physical quantities that affect both productivity and workers' safety [5]. Thus, the new family of smart objects (SOs) can be introduced with their peculiar characteristics. They are conventional objects, devices, or tools equipped with sensors, electronics, and proper communication protocols to sense and measure, collect and exchange data with other devices or users, who can remotely supervise the industrial systems through existing networks.

Many applications can be found in literature aiming, for example, to monitor safety, hazardous events and climate changes for workers thanks to a smart helmet [6]. Maintenance, repair, and operations of parts inventory and predictive maintenance (PdM) can go well with the integration of sensors on the equipment (consumables, maintenance supplies, spare parts, and machines) involved in the process (mechanical processing, chemical plants, energy production) to predict failures. Implementing these monitoring systems could reduce maintenance and repair costs, extend equipment lifecycle, and help workers to stay safe in the working environment. PdM will strongly benefit from this revolution since it will be possible to predict failure events, achieving a real-time monitor of the stress-strain behavior of a part involved in the production process [7].

Given the wide variety of applications and the difficulty of implementing standard solutions, highly customized solutions for measuring relevant physical quantities and exchanging information could be preferred in this context. In this kind of context, printed electronics (PE) can assume the central role in transforming objects from conventional into smart thanks to a new class of sensors and electronics customizable according to application and object. PE can fabricate sensors intended for harsh environments applications (extreme temperatures, corrosive or hazardous substances, etc.) [8] or installed in areas with limited access due to the size of the components involved (turning, milling, and other mechanical tools). One of the appealing advantages (low production costs, flexibility in design, and high variety of materials) of PE technologies is the fabrication of sensors and electronics directly on the objects, simplifying the installation of electronics on existing objects avoiding surface preparation, assembly, or gluing. In the near future, the realization of functional electronic elements on 3D devices will lead to unprecedented scalability, miniaturization, and conformability (with great attention to material compatibility), increasing the functionality of new products [9]. Moreover, PE can be easily integrated into the process flow of additive manufacturing technologies to produce prototypes and SOs. The combination of AM with PE will allow us the rapid production of aids, functional prototypes, and even objects not available on the market [10] and made "smart" by integrating sensors and electronics during fabrication.

Aerosol jet printing (AJP) can play an important role in this context. It is a material-jet additive manufacturing technique, which sees its process composed of aerodynamic focusing of liquid particles (without the use of masks) on different types of substrates. AJP goes beyond the typical shortcomings of PE technologies, such as nozzle clogging, the coffee-ring effect of droplets, and the limited viscosity range of inks. In addition, AJP can print indifferently on non-planar substrates and complex 3D surfaces, enabling the fabrication of sensors and custom electronics on each surface in a controlled manner, quickly and by contacting parts without the use of wires and glue [11].

In this work, we aim to analyze the opportunities of AJP for fabricating sensors directly on the objects. Section 2 will define typical architectures for SOs, Section 3 will present some sensors (piezoelectric sensor, strain gauges, temperature sensors) and a printed antenna developed through the above technologies, while Section 4 will discuss the technologies by making a comparison and defining possible future perspectives.

II. Smart Object Architectures

A smart object can be defined as a device that keeps its original design functionalities, but it is also capable of measuring physical quantities (temperature, humidity, mechanical deformations, etc.) thanks to embedded sensors, and of elaborating information thanks to embedded electronics. Such information can be used to perform autonomous decisions or can be shared with other devices, operators [1] or cloud servers, where data mining and machine learning algorithms can remotely perform diagnosis, optimize and reconfigure intelligent product lines [12]. The great advantage in using SOs relies upon their wireless communication and also no cables are required to supply the electronics for most of the applications. SOs can be divided into two great families, active and passive. Fig. 1 presents the block diagram describing the two architectures.

A. Active Smart Objects

An active SO is equipped with a series of electronic parts. First of all, one or more sensors must be implemented to measure physical quantities. Depending on the type of sensor, there must be a sensor interface to read the data and pre-process the output. The processing unit can be a microcontroller or another programmable system and will be responsible for the transformation of the measurements into data to be stored and/or shared. The wireless transceiver can be considered as an antenna with a specific protocol to communicate with the network through the gateway. The Cloud/Internet block is responsible to perform the last connection between smart objects, devices, users, and/or machines with the industrial control system,

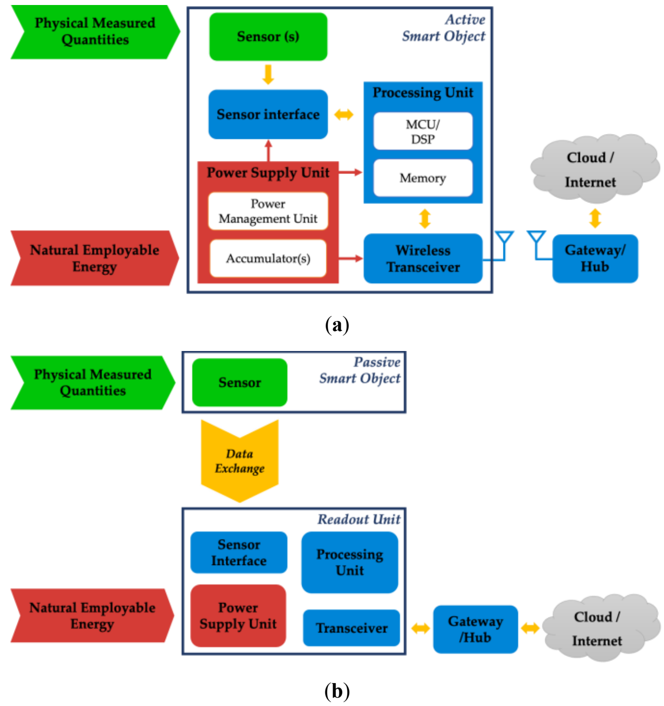

Fig. 1. Block diagrams of (a) active smart object (*b*) and passive smart object.

permitting access and store data. The power unit is essential to provide power to the entire system, and it can be batteries or energy storage units. Energy harvesting could also be a possible alternative to avoid maintenance aspects and exploiting wasted energy present in the environment (thermal energy, kinetic energy, solar power, etc.) [13]. This part must be properly designed since one of the SOs requirements is to minimize power consumption.

B. Passive Smart Objects

Passive SOs can be considered as the best solution when is not possible to perform a local data elaboration because of application constraints. In such a situation, passive components and sensors must be considered, together with an external readout unit for data acquisition and processing. All these aspects are depicted in Fig. 1b. This kind of telemetric system employs passive wireless communication, exploiting a different kind of link like an electric-magnetic, optic, or acoustic one. In this case, the great advantage relies on the absence of a power supply unit for the passive SO, which can be placed in harsh or hermetic environments, but the distance between the two inductors must be lower than few centimeters. For example, a telemetric system was adopted to monitor furnaces or pipes of a heating plant. The readout unit also acts as a bridge between the passive device and the factory network [14].

III. Printed sensors for Smart Object

A. PVDF Printed Sensors for Active Smart Object

Through AJP, it was possible to make a piezoelectric sensor directly on a 3D paper surface. This was made possible by employing materials that are well-matched to paper, a low-temperature substrate that cannot be treated with traditional oven sintering. Piezoelectric polymer polyvinylidene difluoride

(PVDF) is the material selected to make the functional material layer, considered for its good mechanical properties like fatigue resistance, creep, and sunlight, high mechanical strength, flexibility, chemical inertness, fast response, and high sensitivity. The layout is shown in Fig. 2a. The first layer was dedicated to silver interdigitated electrodes manufacturing, then sintered via FLA. A constraining wall was printed using the photopolymer NOA-81 to mark the area dedicated to the piezoelectric ink. Once designed and printed the interdigitated electrodes, the functional PVDF layer was obtained with ten depositions, each one interleaved by curing in a vacuum oven 10 minutes at 75 °C to achieve solvent evaporation and by second curing for 10 minutes at 110 °C to fix the polymeric material. A third step was performed only after ten depositions, a final curing step for 5 minutes at 135 °C.

Electrical and geometrical evaluations were performed, resulting in electrical resistance of 1.77 Ω considering the longest path for each electrode, a thickness of 16 µm and 31.2 µm and a line width of 306.6 µm and 413.6 µm were achieved, respectively for Ag ink and NOA-81. The polarization of the piezoelectric layer was done considering a temperature of 130 °C for half an hour and then a cooling phase keeping applied different voltages for different sensors. The electrical capacitance measurements showed differences caused by the presence of the PDVF layer and its condition. A mean value of 2.58 pF was obtained for the only electrode, a mean value of 2.98 pF after PVDF sintering, and a mean value of 4.07 pF after polarization. The capacitance change within a range of temperatures 20 °C – 90 °C against temperature was evaluated by using a hot plate and by measuring the surface temperature. The capacitance decreased by 1.65 % with respect to the initial value at 20 °C, regardless of the presence of the PDVF layer.

The sensors were then tested by applying increasing masses from 50 to 500 g perpendicular to their surface using a custom structure to determine their impact behavior. The sensors exhibited a linear behavior with increasing recorded voltages in the presence of an increasing mass. Nevertheless, it was not possible to show an increase of the same amount at each step. Moreover, as can be seen from Fig. 2b some points of the curve are confused with each other, due to a non-homogeneous functional layer that may have led to imbalances in the distribution of electric dipoles.

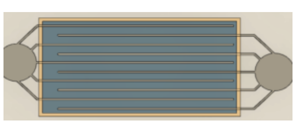

(a)

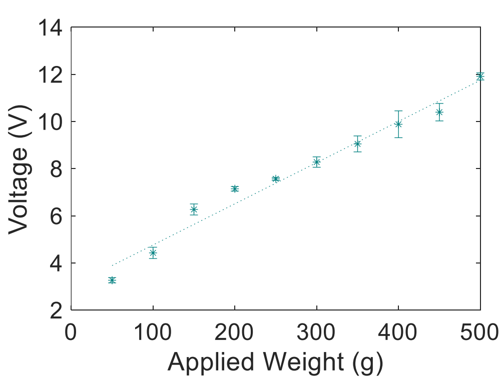

(b)

Fig. 2. (a) PVDF printed sensor layout and (b) results after impact tests, with layout magnification. The dashed line is the straight line that best fits the measured data, obtained by using the method of least square.

B. *AJ printed Strain Gauge*

We fabricated a silver-based strain sensor with high stretchability by using AJP and we investigated its electrical properties. We selected DuPont™ PE873 stretchable ink as silver-based ink since it was properly formulated for stretchable electronics, and DuPont™ Intexar™ TE-11C, a thermoplastic polyurethane (TPU) based film, as substrate. We employed TPU because of its high elasticity, good tensile strength, excellent resistance to fatigue, and biocompatibility. The sensor was designed as a 15-mm long stripe with the aid of AutoCAD software (Autodesk Inc.). The silver ink with its corresponding thinner (PE 8260) was deposited on Intexar™ TE-11C film according to the drawn pattern. The AJP process parameters were set to obtain an average width of 140 µm, and we used a 200 µm nozzle tip. In addition, the AJ printer was configured with a pneumatic atomizer. After the printing phase, all the samples have been cured at 130 °C in a dry oven for 15 minutes. The electrical contacts between terminals of the stripe and the wires were obtained by a 2-part Conductive Epoxy as shown in Fig. 3.

Ink adhesion to the substrate is a necessary condition for the electrode to work correctly. We evaluated the adhesion of the ink through the cross-cut tape test, which is described in the standard ASTM D3359 [15]. First, the samples were cut deep, up to the substrate, according to a straight lattice pattern, to form a grid. Then, after brushing the surface of interest with a brush pen, the grid was covered with a piece of tape. Finally, the tape was rapidly removed, and we observed how the grid looked like, comparing its aspect with the examples provided by the normative. Silver ink on TPU-based film exhibited strong adhesion (Grade-5B).

The width and the thickness were measured with an optical profilometer, and they resulted in 140 µm and 100 µm, respectively. The resistance of the stripe resulted in 10 Ω, according to the sheet resistance declared in the datasheet.

The sensitivity of the printed sensor was evaluated by using the experimental setup already discussed in [16]. Briefly, the ends of the substrate were clamped and were moved by a linear motor to induce a strain, controlling the position. We applied different strain levels, (1%, 3%, 5%, and 7%), maintaining the reached position for 1 minute after each step. We measured the sample electrical resistance with a 6½-digits multimeter (Agilent 34401A), in a two-point probe configuration. Either motor control and real-time acquisition of data about displacement and resistance were guaranteed by a LabVIEW Virtual Instrument (VI) executed by a personal computer (PC). The results are shown in Fig. 4. The resistance change is normalized on the initial value when the deformation is not

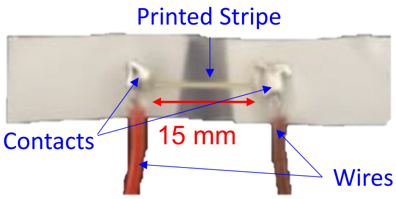

Fig. 3. Silver-based strain sensor for high levels of strain

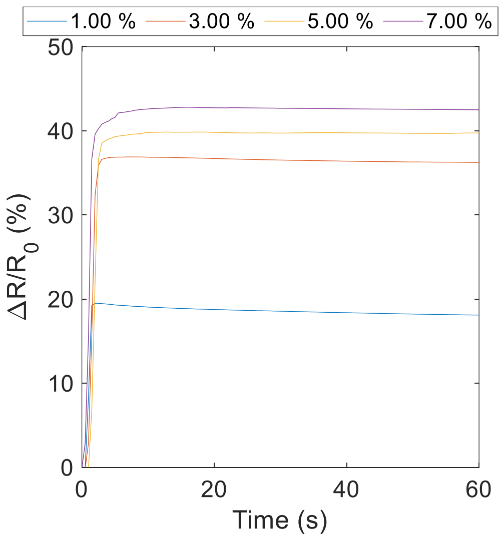

Fig. 4. Strain sensor response for different strain levels.

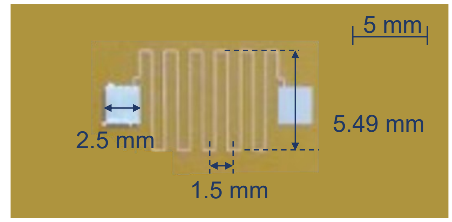

(a)

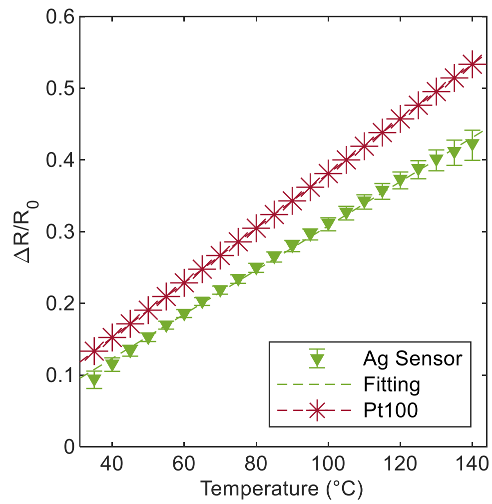

(b)

Fig. 5. Temperature sensor. (a) Picture of the printed 66-mm long sensors. (b) Normalized resistance vs. temperature of the silver sensor (66 mm long) and Pt100 sensor. R_0 is the resistance at 0 °C. Error bars correspond to the output range of eight different sensors.

induced in the sensor. As expected, the resistance change drifts over time, especially for low strain levels. The drift is less than 1%, after 1 minute. Furthermore, the dependence of the normalized resistance change on the strain is not linear: while a strain of 1 % induces a resistance change of 18%, a strain of 7% causes a resistance change of 42%. We tested also the maximum strain level for the silver ink: the conductive path along the stripe was broken when the strain was 17%, while the substrate can withstand elongation up to 40 %.

This sensor could be combined with a telemetric system to realize a passive SO. Otherwise, it can also be coupled with devoted electronics, microprocessors, and antennas for realizing an active smart device.

C. *AJ printed Resistance Temperature Detector*

A silver nanoparticles ink and polyimide foils were employed in the manufacturing of resistance temperature detectors (RTDs) using AJP. Serpentines were designed considering three different lengths (33, 66, 99 mm, Fig. 5a). Two consecutive depositions were realized followed by an oven sintering at 200 °C for 10 minutes. Sensors were tested in terms of adhesion by an adhesion tape test. To test the stability of the sensors up to 400 °C, the sensors were spray-coated with a specific protecting layer able to resist until 450 °C, followed by the deposition of a conductive paste applied on pads for electrical contact with wires. Three consecutive thermal cycles at 400 °C for 30 minutes were performed. Electrical resistance was measured right after the sintering process and each thermal treatment, evidencing a decrease by 40% after the thermal cycles on average to that after the printing process. In particular, 33-mm long sensor, 66-mm long sensor, and 99-mm long sensor measured (17 ± 2) Ω, (40 ± 5) Ω and (60 ± 6) Ω, respectively. The sensors were characterized in a controlled temperature oven, considering a Pt100 as feedback, aiming to define the α coefficient of the sensors in the range 35-140 °C. From Fig. 5b, the overall α coefficient was measured thanks to the slope of the best fit straight line (red line) and resulted as 0.00315 K^{-1}, slightly lower than bulk silver (α = 0.00380 K^{-1}) and the one of Pt100 feedback (α = 0.00385 K^{-1}).

Also these sensors are promising for a possible telemetric system to realize a passive SO. Otherwise, they can also be coupled with devoted electronics, microprocessors, and antennas for realizing active smart devices.

D. *AJ printed Antenna*

In the final example, AJP was used to manufacture a sensing coil and a tuning capacitor to be used in a passive telemetric system for the measurement of resistive sensors at a fixed frequency. In this measuring system, the resistive sensor to be measured is connected to a tuning capacitor and a sensing coil, magnetically coupled with an external readout element. The resistance R_x of the coupled sensor is determined by measuring

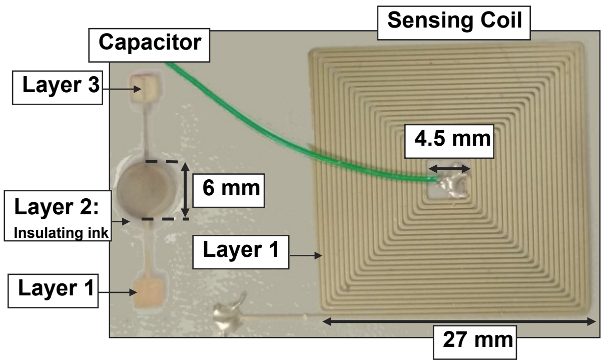

Fig. 6. Printed capacitor and antenna.

the impedance Z at the readout terminals. The components were designed to present a self-resonant frequency of 12.45 MHz, compatible with the most typical impedance analyzers. At this frequency, the electronic components could be modeled with lumped elements. It must also be noted that the distance between the coils plays an important role in the amplitude of Re(Z): the greater the distance the lower the sensitivity of the system. Some assumptions were made to simplify Re(Z) formula: R_x is greater than 1 kΩ, sensing resistance R_2 is negligible being lower than some tens of ohm, the distance between coils is fixed and the frequency of the readout part (f_{r1}) is greater than the one of the sensing part (f_{r2}) to ensure good sensitivity. These considerations allowed us to calculate R_x from equation (1) to (5).

Thanks to the conductive ink, the inductor and bottom electrode of the capacitor were printed by AJP and sintered in an oven following a thermal treatment of 1 h at 150 °C (Layer 1). This step was followed by UV insulators printing and UV curing, performed right after the deposition (Layer 2). The last printing phase regarded the deposition of the upper electrode, followed by the same thermal treatment performed in the first step (Layer 3). Fig. 6 shows the final products.

The printed components were geometrically characterized by measuring the thickness and the width of the tracks and they were electrically tested by measuring their electrical impedance. On average, the thickness (t) and width (w) of the inductor tracks were found to be 3 µm and 260 µm, respectively, while the total resistance was 87 Ω (R_2). According to the results, we obtained the resistivity ρ of the silver ink equal to 4.6 µΩ·cm by applying the formula $\rho = R_2 \cdot w \cdot t/l$, where l, which is the total path length of the inductor, is 0.143 m, according to the inductor design. The printed capacitance (C) was found to be (14.0 ± 0.2) pF due to the insulator thickness (d) of 65 µm. The relative permittivity ε_r was found to be 3.62 by applying $\varepsilon_r = C \cdot A/(d \cdot \varepsilon_0)$, where area A is 28 mm^2 and ε_0 is the vacuum permittivity.

The printed coil and the capacitor were validated in a telemetric system properly designed to measure resistive loads. The printed components were connected in parallel to different commercial resistors of known value to emulate a resistive sensor. A readout inductor (copper tracks on a substrate of FR4 glass-reinforced epoxy) with the same characteristics of the printed inductor was placed parallel and opposite to the printed coil at a distance of 4 mm. One resistor of 5606 Ω was used to calibrate the system and to estimate β by using (5). From the experiment, we obtained β equal to 6.36 µH. Then the telemetric system was validated with other seven resistors and we obtained a maximum error between the nominal value and the measured value lower than 2.28 % in the range 2.2 kΩ and 27 kΩ. The comparison between the estimation of R_x obtained by using the proposed method and the nominal resistance is shown in Fig. 7. The results proved the possibility to print antennas and capacitors that can be used to measure resistor, which can be also fabricated by AJP as described in the previous sections, and to design a passive SO.

$$R_x = \frac{L_2(Re(Z(f_w)) - R_1)}{\beta - C_0 \cdot R_2 \cdot (Re(Z(f_w)) - R_1)} \quad (1)$$

$$Re(Z(f_w)) = \frac{\beta \cdot R_x}{L_2 + R_x \cdot C_0 \cdot R_2} + R_1 \quad (2)$$

$$f_w = f_{r2} = \frac{1}{2\pi\sqrt{L_2 \cdot C_0}} \quad (3)$$

with

$$C_0 = C_x + C_2 \quad (4)$$

$$\beta = \frac{L_M^2}{L_2 \cdot n^2} = (Re(Z(f_w)) - R_1)\left(\frac{L_2}{R_x} + C_0 \cdot R_2\right) \quad (5)$$

CONCLUSIONS

The impetus generated by the fourth industrial revolution is gradually leading to a change in the conception of a manufacturing process. The possibility of employing "smart" objects able to perceive changes in the environment, measure physical quantities through sensors, and share the acquired data wirelessly with other smart objects and with industrial management systems will allow reaching new heights in terms of efficiency, optimization, and flexibility. Fabricating smart objects is possible because objects can be functionalized by making them capable of collecting information and communicating it while maintaining their usual purpose in the work environment. Therefore, soon, specific new technologies for embedding sensors on objects will be required. In this work, smart objects have been classified into active and passive smart objects obtained by AJP. AJP is suitable for customization

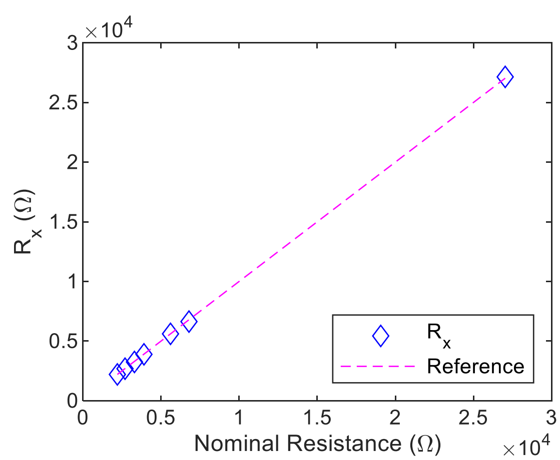

Fig. 7. Validation of the telemetric system by changing the value of Rx. On x-axis the measured values by means of a multimeter, on y-axis Rx calculated by applying (1).

thanks to its flexibility regarding the printing process, design, and ink selection. Specifically, temperature sensors, strain gauges, and piezoelectric sensors described in this work were fabricated to test the feasibility of common sensors for integration into smart objects. In the future, the goal is to target the metrological performance of the sensors by subjecting them to various working conditions (operating temperature and humidity ranges, stress conditions, etc.). Furthermore, AJP could be a rapid method to assess the compatibility of the manufacturing process with specific objects (surface shape, material requirements, etc.). AJP has shown promise as technology for making traditional objects "smart". Indeed, PE could offer low-cost and accessible manufacturing processes. Further researches on newer PE technologies are still needed to achieve large-scale smart object manufacturing.

REFERENCES

[1] G. Kortuem, F. Kawsar, V. Sundramoorthy, and D. Fitton, "Smart objects as building blocks for the internet of things," *IEEE Internet Comput.*, vol. 14, no. 1, pp. 44–51, Jan. 2010, doi: 10.1109/MIC.2009.143.

[2] S. Munirathinam, "Industry 4.0: Industrial Internet of Things (IIOT)," in *Advances in Computers*, vol. 117, no. 1, Academic Press Inc., 2020, pp. 129–164.

[3] M. O. Gokalp, K. Kayabay, M. A. Akyol, P. E. Eren, and A. Koçyiğit, "Big Data for Industry 4.0: A Conceptual Framework," in *2016 International Conference on Computational Science and Computational Intelligence (CSCI)*, 2016, pp. 431–434, doi: 10.1109/CSCI.2016.0088.

[4] T. Ruppert, S. Jaskó, T. Holczinger, and J. Abonyi, "Enabling Technologies for Operator 4.0: A Survey," *Appl. Sci.*, vol. 8, no. 9, 2018, doi: 10.3390/app8091650.

[5] Y. Cohen, M. Faccio, F. Pilati, and X. Yao, "Design and management of digital manufacturing and assembly systems in the Industry 4.0 era," doi: 10.1007/s00170-019-04595-0.

[6] T. Eldemerdash et al., "IoT Based Smart Helmet for Mining Industry Application," *Int. J. Adv. Sci. Technol.*, vol. 29, no. 1 SE-Articles, pp. 373–387, Jan. 2020, [Online]. Available: http://sersc.org/journals/index.php/IJAST/article/view/3004.

[7] I. Perez-Alfaro, D. Gil-Hernandez, O. Muñoz-Navascues, J. Casbas-Gimenez, J. C. Sanchez-Catalan, and N. Murillo, "Low-Cost Piezoelectric Sensors for Time Domain Load Monitoring of Metallic Structures During Operational and Maintenance Processes," *Sensors*, vol. 20, no. 5, 2020, doi: 10.3390/s20051471.

[8] A. S. Almuslem, S. F. Shaikh, and M. M. Hussain, "Flexible and Stretchable Electronics for Harsh-Environmental Applications," *Adv. Mater. Technol.*, vol. 4, no. 9, p. 1900145, Sep. 2019, doi: 10.1002/admt.201900145.

[9] Y. Gu, D. Park, S. Gonya, J. Jendrisak, S. Das, and D. R. Hines, "Direct-write printed broadband inductors," *Addit. Manuf.*, vol. 30, p. 100843, Dec. 2019, doi: 10.1016/j.addma.2019.100843.

[10] D. J. Horst, C. Duvoisin, and R. D. A. Vieira, "Additive Manufacturing at Industry 4.0: a Review," *Artic. Int. J. Eng. Tech. Res.*, vol. 8, no. 8, p. 3, Sep. 2018, [Online]. Available: www.erpublication.org.

[11] B. Clifford, D. Beynon, C. Phillips, and D. Deganello, "Printed-Sensor-on-Chip devices – Aerosol jet deposition of thin film relative humidity sensors onto packaged integrated circuits," *Sensors Actuators B Chem.*, vol. 255, pp. 1031–1038, Feb. 2018, doi: 10.1016/j.snb.2017.08.086.

[12] M. Saqlain, M. Piao, Y. Shim, and J. Y. Lee, "Framework of an IoT-based Industrial Data Management for Smart Manufacturing," *Journal of Sensor and Actuator Networks*, vol. 8, no. 2. 2019, doi: 10.3390/jsan8020025.

[13] A. Pop-Vadean, P. P. Pop, T. Latinovic, C. Barz, and C. Lung, "Harvesting energy an sustainable power source, replace batteries for powering WSN and devices on the IoT," *IOP Conf. Ser. Mater. Sci. Eng.*, vol. 200, p. 012043, May 2017, doi: 10.1088/1757-899X/200/1/012043.

[14] M. Bona, M. Borghetti, E. Sardini, and M. Serpelloni, "Telemetric Technique for Passive Resistive Sensors Based on Impedance Real Part Measurement at Fixed Frequency," *IEEE Trans. Instrum. Meas.*, vol. 67, no. 9, pp. 2160–2168, 2018, doi: 10.1109/TIM.2018.2811279.

[15] "ASTM D3359: Standard test methods for measuring adhesion by tape test."

[16] M. Borghetti, M. Serpelloni, E. Sardini, and O. Casas, "Multisensor system for analyzing the thigh movement during walking," *IEEE Sens. J.*, vol. 17, no. 15, pp. 4953–4961, 2017, doi: 10.1109/JSEN.2017.2715857.